How the Structure of an Adenine Tract Depends on Sequence Context: A New Model for the Structure of T_nA_n DNA Sequences†

Mary Ann Price‡ and Thomas D. Tullius*

Department of Chemistry, The Johns Hopkins University, Baltimore, Maryland 21218

Received May 1, 1992; Revised Manuscript Received October 21, 1992

ABSTRACT: We present a new model to explain the bending and local structural properties of T_nA_n sequences in DNA. Current models suggest that an adenine tract has the same unusual structure when found in a T_nA_n sequence as it has when surrounded by mixed-sequence B-DNA. On the basis of hydroxyl radical cleavage patterns of several T_nA_n sequences, we instead propose that the T_2A_2 or T_3A_3 core of such sequences is B-DNA-like but that adenines and thymines outside of this core, if sufficient in number, can form the unusual structure adopted by adenine tracts surrounded by mixed sequence DNA. We pursued further the structure of $T_7A_7N_7$, a molecule which exhibits reduced electrophoretic mobility on native polyacrylamide gels and is therefore presumed to be bent. We attempted to mimic the structure of $T_7A_7N_7$ that was predicted by our model by designing two new sequences, one in which the T_3A_3 core of $T_7A_7N_7$ is substituted by six nucleotides of mixed sequence (N_6) and the other in which the T_2A_2 core is replaced by N_4. Hydroxyl radical cleavage patterns of all three molecules are nearly indistinguishable. All three molecules run anomalously slowly on a native polyacrylamide gel, with the mobility of $T_4N_6A_4N_7 > T_7A_7N_7 \approx T_5N_4A_5N_7$. Analysis of the hydroxyl radical cutting pattern of $T_7A_7N_7$ by Fourier transformation reveals the occurrence of an unusual structure at intervals of ~10 bp, a periodicity which is not evident in the sequence of the DNA.

Since the discovery that kinetoplast DNA migrates more slowly on a polyacrylamide gel than would be expected for its length (Marini et al., 1982), there has been much interest in the ability of DNA to bend. The key original observation was that bending in kinetoplast DNA is associated with the presence of several short runs of adenines that occur once per DNA helix repeat (Marini et al., 1982; Wu & Crothers, 1984; Diekmann & Wang, 1985). This insight led to the use of synthetic oligonucleotides to investigate the sequence dependence of DNA bending. It was found that sets of at least four contiguous adenines, phased to occur every 10–11 base pairs (bp),[1] are needed to achieve measurable bending (Hagerman, 1985; Koo et al., 1986; Diekmann, 1986) and that poly(dA)·poly(dT) is not bent (Koo et al., 1986).

The mere presence of phased adenine tracts does not always lead to bending, though. The sequence context within which adenine tracts occur can affect the degree to which DNA bends. In the most striking example, Hagerman (1986) showed that the sequence $(CGA_4T_4)_n$ runs on a gel as if it were bent but its sequence isomer $(CGT_4A_4)_n$ migrates with straight DNA.

Most experiments aimed at understanding the phenomenon of DNA bending use an assay, like gel mobility, that is sensitive to the overall shape of the DNA molecule. Other work has addressed the structural details of bent DNA at the nucleotide level, and how the structure differs from that of straight DNA. For example, the hydroxyl radical cleavage pattern of kinetoplast DNA is remarkably different from that of mixed-sequence DNA (Burkhoff & Tullius, 1987). The most unusual feature is that the extent of cleavage decreases smoothly along an adenine tract from 5′ to 3′ and then increases in the sequences that separate the A-tracts. Other experiments also have detected nonuniformity of structure along adenine tracts. For example, most of the thymines in a T-tract are protected from UV-induced thymine dimer formation, except for the thymines at the 3′ end of the tract (Lyamichev, 1991).

Because in kinetoplast DNA there are several phased adenine tracts, the overall hydroxyl radical cleavage pattern resembles a sine wave. The unusual cutting pattern of kinetoplast DNA is consistent with models that attribute bending to the unusual structure of adenine tracts.

$(CGA_4T_4)_n$, like other bent sequences, has the distinctive hydroxyl radical cleavage pattern of kinetoplast DNA (Burkhoff & Tullius, 1988). In sharp contrast, $(CGT_4A_4)_n$ has a cleavage pattern much like that of straight, mixed-sequence DNA.

Some models that attempt to account for the normal gel mobility of $(CGT_4A_4)_n$ posit that these adenine tracts take on the same structure as in DNA that is bent but that the discontinuities in structure that normally lead to curvature in repeats of A-tracts are poorly phased in this sequence (Ulanovsky & Trifonov, 1987; Koo & Crothers, 1988). The destructive interference of these out-of-phase structural anomalies causes the DNA to appear by gel mobility to be straight instead of bent. Hydroxyl radical cleavage data for these sequences (Burkhoff & Tullius, 1988) provided evidence for a different model that the two isomeric sequences in fact

† This research was supported by USPHS Grant GM 40894. M.A.P. was a predoctoral fellow of the National Science Foundation. T.D.T. is a research fellow of the Alfred P. Sloan Foundation, a Camille and Henry Dreyfus Teacher–Scholar Awardee, and the recipient of a Research Career Development Award from the National Cancer Institute of the NIH (CA 01208). We gratefully acknowledge the use of densitometry instrumentation maintained by the Institute for Biophysical Research on Macromolecular Assemblies at Johns Hopkins, which is supported by an NSF Biological Research Centers Award (DIR-8721059) and by a grant from the W. M. Keck Foundation.

* To whom correspondence should be addressed.

‡ Present address: Imperial Cancer Research Fund, Lincoln's Inn Fields, London WC2A 3PX, U.K.

[1] Abbreviations: bp, base pair(s); EDTA, ethylenediaminetetraacetic acid; NMR, nuclear magnetic resonance; R_L, relative gel mobility; TE buffer, 10 mM Tris·HCl/0.1 mM EDTA (pH 8.0); Tris, tris(hydroxymethyl)aminomethane.

0006-2960/93/0432-127$04.00/0

have different structures. On the basis of these data, it was postulated that steric clash at the central TA step of T_4A_4 interferes with the propeller twisting that is associated with the narrow minor groove of A-tracts in kinetoplast and other bent DNAs (Wing et al., 1980; Drew & Travers, 1984; Burkhoff & Tullius, 1987; Nelson et al., 1987), and also in poly(dA)·poly(dT)(Behling & Kearns, 1986; Alexeev et al., 1987).

Differential scanning calorimetric measurements (Park & Breslauer, 1991) offered further support for the idea that $T_4A_4N_2$ does not adopt the unusual structure that is characteristic of bent DNA. This sequence does not undergo the unusual premelting transition that is seen for $A_4T_4N_2$ and for other runs of adenine (Herrera & Chaires, 1989; Chan et al., 1990). Measurements of imino proton exchange by NMR (Leroy et al., 1988) also provided evidence that A·T base pairs in bent DNA adopt a different structure from A·T base pairs in straight DNA.

The idea that T_4A_4 takes on a B-DNA-like structure might suggest that T_nA_m sequences of any length are straight. Haran and Crothers (1989) tested this prediction using gel mobility as the assay for bending. Since they found that $(TA_5N_4)_n$ is bent, it is clear that a single TA step to the 5′ side of an A-tract is incapable of abolishing bending. Furthermore, longer T_nA_n tracts [in particular, $(T_7A_7N_7)_n$] were shown to be bent. Haran and Crothers (1989) explained the differences in the bending properties of various T_nA_n sequences in the context of the model that an A-tract in a T_nA_n block has the same structure as an A-tract surrounded by mixed-sequence DNA. According to this model, whether or not an A-tract-containing DNA is bent depends on the phasing of the small bends that are formed at A_n–B (where B designates B-form DNA), B–T_n, and T_n–A_n junctions (Koo & Crothers, 1988; Haran & Crothers, 1989).

We have used the hydroxyl radical cleavage experiment to examine the structures of several T_nA_n sequences at the nucleotide level, to complement the gel mobility studies that test for global bending. This method permits us to test the hypothesis that the structures of all adenine tracts are similar, regardless of whether the DNA is bent or straight. We use our data to construct a new model for the structures of T_nA_n sequences. This model includes structural features revealed by the hydroxyl radical cutting patterns, and also accounts for the gel mobility data.

MATERIALS AND METHODS

Cloning of T_nA_n Sequences. We synthesized the sequences listed in Figure 1A, and their complements, with AATT overhanging ends and cloned them into the *Eco*RI site of plasmid pUC18. The sequences were designed so that the *Eco*RI site is destroyed upon insertion. The oligonucleotides were synthesized using phosphoramidite chemistry (Biosearch 8600 DNA synthesizer; Cruachem reagents) and purified by electrophoresis on a denaturing polyacrylamide gel, or by elution through an oligonucleotide purification cartridge (Applied Biosystems). To form duplex DNA, an oligonucleotide and its complement were mixed at a 1:1 ratio in 10 mM Tris·HCl/0.1 mM EDTA (pH 8.0) (TE buffer) with 0.1 M NaCl, heated to 70 °C, and slowly cooled. The duplex was then coprecipitated with 0.2 μg of *Eco*RI-digested vector DNA, at a molar ratio of 1:10–200 vector to insert. The mixture was ligated overnight at 4 °C, cut with *Eco*RI for 1–2 h to linearize any vector not containing insert, and transformed into *Escherichia coli* TG1 or DH5α cells. Clones were sequenced by the Sanger method (Sanger et al., 1977) with

A

A_5N_5	aattgga(GGCAAAAAT)$_4$ggtcc
$T_3A_3N_6$	aattggag(AGTTTAAACT)$_4$ctcc
$T_4A_4N_2$	aattgga(CGTTTTAAAA)$_4$cgtcc
$T_5A_5N_{11}$	aattgga(GGCCTTTTTAAAAACCGGGCC)$_2$tcc
T_5A_5	aattggc(TTTTTAAAAA)$_3$gcc
	aattggaa(TTTTTAAAAA)$_4$ttcc
$T_7A_7N_7$	aattgga(GGCCTTTTTTTAAAAAAACCC)$_2$tcc
$T_4N_6A_4N_7$	aattgga(GGCCTTTTGTATACAAAACCC)$_2$tcc
$T_5N_4A_5N_7$	aattgga(GGCCTTTTTGTACAAAAACCC)$_2$tcc

B

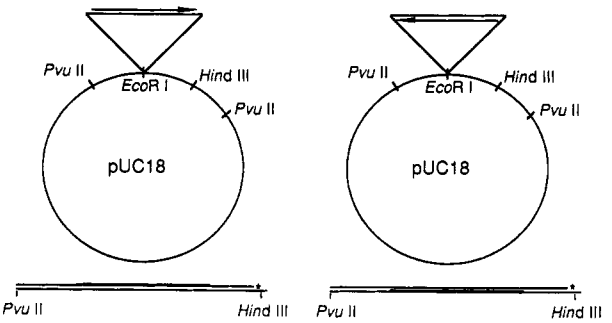

FIGURE 1: (A) Sequences of adenine tract oligonucleotides. Sequences are written from 5′ to 3′. To the left of each sequence is the shorthand designation that is used throughout this paper. (B) Plasmid constructs and resulting restriction fragments. Each oligonucleotide was annealed to its complement and cloned into the *Eco*RI site of pUC18 (see Materials and Methods). Schematics of plasmids containing the two possible orientations of the inserted sequences are shown. The arrow above the construct represents the sequences listed in (A); the arrowhead is placed at the 3′ end of the sequence. Shown below the constructs are the resulting 3′-radiolabeled *Pvu*II–*Hin*dIII restriction fragments for each orientation of the insert. The thick line represents the sequences shown in (A).

Sequenase 2.0 (United States Biochemical), or by use of the Maxam–Gilbert sequencing reactions (Maxam & Gilbert, 1980). Clones containing the two orientations of an insert sequence were selected for further study. Figure 1B shows a diagram of the resulting constructs.

Hydroxyl Radical Cleavage Experiments. DNA prepared by the alkaline lysis miniprep procedure (Maniatis et al., 1982) was 3′ radiolabeled by standard methods at the *Hin*dIII site using [α-^{32}P]dATP (Maniatis et al., 1982). The hydroxyl radical cleavage reaction (Tullius & Dombroski, 1985) typically was carried out on a radiolabeled *Hin*dIII–*Pvu*II restriction fragment (10 000–30 000 dpm) dissolved in 70 μL of a buffer consisting of 14.3 mM Tris·HCl/14.3 mM NaCl (pH 8). The final concentrations of the cutting reagents were 50 μM Fe^{2+}, 100 μM EDTA, 0.03% H_2O_2, and 1 mM sodium ascorbate, in a total volume of 100 μL. Reactions were stopped after 1 min by adding 100 μL of a solution containing 0.0135 M thiourea, 0.0135 M EDTA, and 0.6 M sodium acetate. DNA was precipitated with ethanol twice, rinsed with 70% ethanol, dried in a SpeedVac concentrator, dissolved in 3 μL of formamide loading buffer, and loaded on an 8% denaturing polyacrylamide sequencing gel [acrylamide:bis(acrylamide) ratio of 19:1]. After electrophoresis, the gel was dried onto filter paper and exposed to preflashed X-ray film (Kodak X-Omat) at room temperature. The autoradiograph of the gel was scanned using a Molecular Dynamics Model 300E densitometer. The ImageQuant software included with the densitometer was used to make a one-dimensional scan along a narrow rectangle encompassing the center of a lane. The

scan was plotted using Microsoft Excel.

Gel Mobility Determination. A DNA sample was prepared for native gel electrophoresis by adding 2 mL of 6× native dye (Maniatis et al., 1982) to 1000 dpm of radiolabeled *Hin*dIII–*Pvu*II restriction fragment in 5 μL of TE buffer. Size markers (1-kb ladder, BRL) were radiolabeled with [α-^{32}P]dATP and [α-^{32}P]dCTP and run in a separate lane on the gel. Samples were electrophoresed on a native 8% polyacrylamide gel [acrylamide:bis(acrylamide) ratio of 29:1] at 250 V at 22 °C until the xylene cyanol marker dye reached 27 cm on the 40-cm-long gel. The gel was dried onto filter paper and exposed to X-ray film. A plot of the mobilities of the size markers versus their length [centimeters migrated vs log (length in bp)] was made, and a straight line was fitted to the data. The apparent lengths of our 282 bp restriction fragments were determined on the basis of their mobility, using the equation of this line.

Fourier Transform Analysis of Cleavage Patterns. The autoradiograph of a gel containing hydroxyl radical cleavage products was scanned with a Joyce-Loebl Chromoscan 3 densitometer, and the peaks were integrated using software included with the instrument. The density of the film away from the lanes containing sample was taken as the background value for integration. Since each different adenine tract sequence was cloned into the same site in the plasmid, the sequences flanking the inserts in each construct were identical. This allowed us to normalize the cleavage intensities of bands within the inserted sequences to the sum of the integrals of seven bands contained in all the constructs, 5′-CCAATTC-3′, located to the 3′ side of the insert. Normalization helped ensure that the height of a Fourier peak would accurately reflect the amplitude of the variation in cleavage. We constructed a data set by repeating in tandem the integrals of the 40 nucleotides in $(A_5N_5)_4$, or the 42 nucleotides in $(T_7A_7N_7)_2$, to give a total of 420 data points. A constant was subtracted from each data set so that the wave in the data oscillated around the origin. We analyzed the resulting data set by Fourier transformation as described (Hayes et al., 1990).

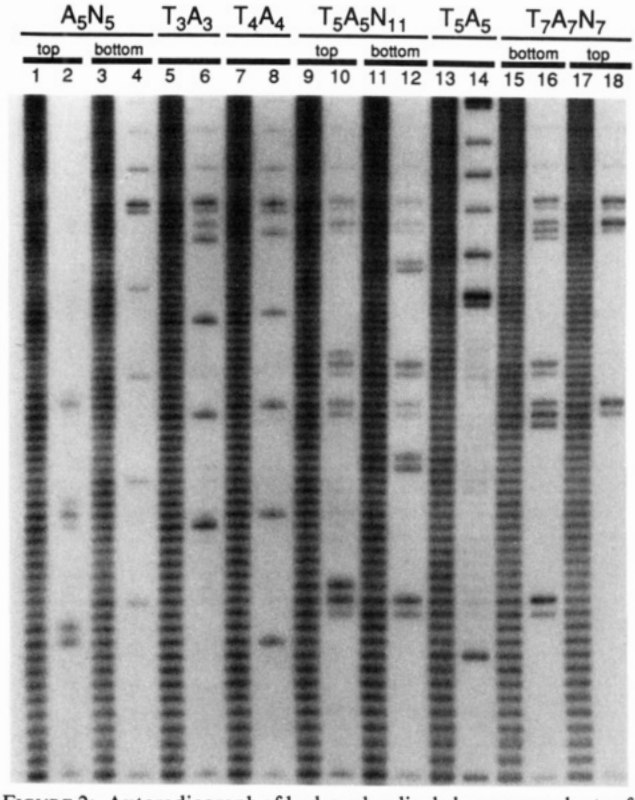

FIGURE 2: Autoradiograph of hydroxyl radical cleavage products of adenine tract DNA. Odd-numbered lanes contain the products of hydroxyl radical cleavage, and even-numbered lanes contain the products of Maxam–Gilbert guanine-specific sequencing reactions for each sequence. For non-self-complementary sequences, *top* refers to the sequence shown in Figure 1A; *bottom* refers to the complementary strand. Lanes 1 and 2 contain the top strand of A_5N_5; lanes 3 and 4, the bottom strand of A_5N_5; lanes 5 and 6, $T_3A_3N_4$; lanes 7 and 8, $T_4A_4N_2$; lanes 9 and 10, the top strand of $T_5A_5N_{11}$; lanes 11 and 12, the bottom strand of $T_5A_5N_{11}$; lanes 13 and 14, $(T_5A_5)_3$; lanes 15 and 16, the bottom strand of $T_7A_7N_7$; lanes 17 and 18, the top strand of $T_7A_7N_7$. The plots shown in Figures 3–5 are scans made from this autoradiograph, with the exception of $(T_5A_5)_4$ in Figure 5B.

RESULTS

Hydroxyl Radical Cleavage Patterns. The autoradiograph of a denaturing gel on which was run the products of hydroxyl radical cleavage of several different adenine tracts is shown in Figure 2. Densitometric scans of lanes on the autoradiograph are presented in Figures 3–5. These hydroxyl radical cleavage experiments were carried out in a buffer containing 10 mM NaCl. Since magnesium is known to affect the electrophoretic mobility of bent DNA (Diekmann, 1987), experiments also were carried out in the presence of magnesium. Cleavage patterns nearly identical to the ones presented here were produced. Since there appeared to be no significant difference in the cleavage patterns in the presence or absence of magnesium, and since no magnesium was added in the gel mobility experiments (Haran & Crothers, 1989) or in the original hydroxyl radical cleavage experiments on adenine tracts (Burkhoff & Tullius, 1987, 1988), we show here only the patterns obtained in the absence of magnesium.

The hydroxyl radical cleavage patterns for the adenine tract, and the complementary thymine tract, of A_5N_5[2] surrounded by mixed-sequence DNA are shown in lanes 1 and 3 of Figure 2, and in Figure 3. $(A_5N_5)_n$ has been found to migrate very slowly on an electrophoresis gel (Koo et al., 1986), and so would be considered to be quite bent by the standard assay. It is useful to note features of the A_5N_5 cleavage pattern that we consider typical of bent DNA, and that also were found in the original experiments on bent kinetoplast DNA (Burkhoff & Tullius, 1987). There is a smooth decrease in cutting along the adenine tract from the 5′ to the 3′ end (from left to right in all of the densitometer traces we show). Within the segment of mixed sequence (N_5), the cutting frequency rises again to the maximum level. The thymine tract has similar features, although the minimum in cutting occurs closer to its 5′ end. The slope of the decrease in cutting in both cases is steep.

Since all of the adenine tract inserts are flanked by the same sequences and were run to the same position on the gel, we use the cleavage patterns of the common flanking sequences as a reference in comparing the cutting patterns of the various adenine tracts to that of A_5N_5. By this means, both the shapes of the cleavage patterns and the intensities of bands may be directly compared among insert sequences. It is important to note that because bands are less well separated at the top of the gel than at the bottom, the variable degree of overlap of bands can cause the perceived steepness of a cleavage pattern to depend on how far the set of bands has migrated. Therefore, it is important that fragments have migrated to approximately

[2] When we use the notation "N" for nucleotides in a sequence, a particular nucleotide sequence is meant (as detailed in Figure 1). "N" does not denote a random nucleotide sequence, but only serves to emphasize that this part of the sequence does not consist of runs of adenines or thymidines.

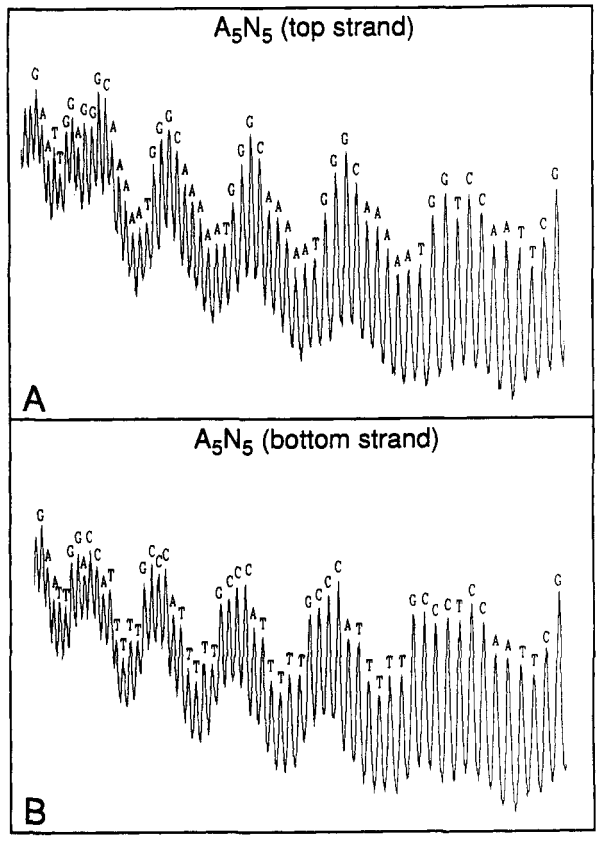

FIGURE 3: Densitometer scans of hydroxyl radical cleavage patterns of the two strands of A_5N_5. All scans read 5′ to 3′ from left to right. Labels on peaks indicate that cleavage occurred at the deoxyribose attached to the designated base. Panel A, scan of the top strand of A_5N_5; panel B, the bottom strand of A_5N_5.

the same extent on the gel for detailed comparisons of cleavage patterns to be made, which our experimental design ensures.

The hydroxyl radical cleavage pattern of $T_4A_4N_2$, a sequence that does not run anomalously slowly on a gel (Hagerman, 1986), is shown in lane 7 of Figure 2, and in panel B of Figure 4. The cutting pattern of this sequence previously was shown to be more like that of mixed-sequence DNA, and not like bent kinetoplast DNA (Burkhoff & Tullius, 1988). We have repeated this experiment here for comparison with the results for A_5N_5 and for the T_nA_n sequences. As found before, the cleavage pattern of $T_4A_4N_2$ is fairly even. In some experiments, $T_4A_4N_2$ showed a very slight decrease in cutting in the adenine tract. However, comparison of the cleavage patterns makes it clear that, in contrast to the large modulations in the pattern of A_5N_5, $T_4A_4N_2$ has a much more regular cleavage pattern.

The cleavage pattern of $T_5A_5N_{11}$, another T_nA_n sequence that by gel mobility does not appear to be bent (Haran & Crothers, 1989), is shown in lanes 9 and 11 of Figure 2, and in panel C of Figure 4. The T_5A_5 tract is cut to a lesser extent compared to the N_{11} sequence. A slight local maximum in cleavage occurs in both repeats at the 3′-T just before the first A.

Next we discuss the cutting pattern of $T_7A_7N_7$, a T_nA_n sequence which by gel mobility is bent (Haran & Crothers, 1989). This cleavage pattern is shown in lanes 15 and 17 in Figure 2, and in panel A in Figure 5. The cutting pattern of $T_7A_7N_7$ is more like that of the bent sequence A_5N_5 than the straight sequence $T_4A_4N_2$, with clear decreases in cleavage in the A-tracts. The TA step at the center and one nucleotide to either side are cut to a greater extent than the rest of the

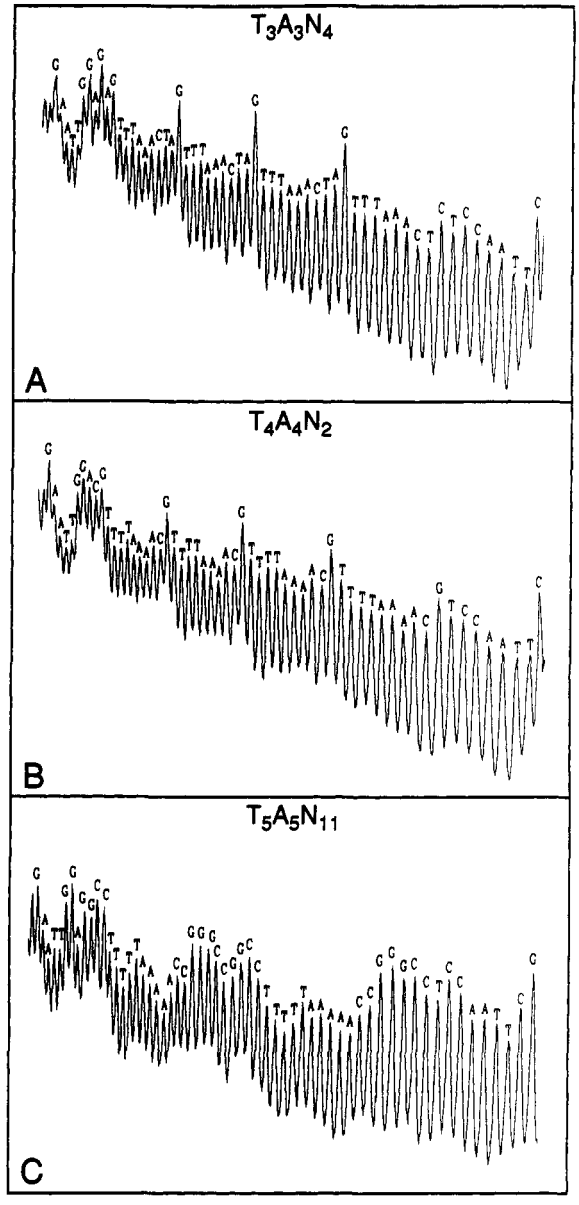

FIGURE 4: Densitometer scans of hydroxyl radical cleavage patterns of straight T_nA_n sequences. Panel A, $T_3A_3N_4$; panel B, $T_4A_4N_2$; panel C, the top strand of $T_5A_5N_{11}$.

T_7A_7 block; decreases in cleavage are found further away from the TA step in both the adenine and thymine tracts. Alternation of regions of decreased cutting with regions of normal cutting (in the N_7 sequence and around the TA step) results in a sinusoidal cutting pattern, with valleys occurring at roughly 10-nucleotide intervals. This periodicity of cutting is interesting, since the sequence repeat of $T_7A_7N_7$ is 21 bp, and the blocks of nucleotides occur in sets of seven. We performed a Fourier analysis of the cutting pattern of the $T_7A_7N_7$ sequence to more quantitatively evaluate the periodicities in the cleavage. We present this analysis below.

Another bent T_nA_n sequence we subjected to cleavage with the hydroxyl radical is $(T_5A_5)_n$ (Hagerman, 1988) (lane 13, Figure 2; panel B, Figure 5). Again we see a pattern having variations in hydroxyl radical cleavage that are reminiscent of the A_5N_5 pattern, rather than the even cutting pattern of $T_4A_4N_2$. Cleavage at and around the TA step occurs to nearly the extent of mixed-sequence DNA, as also was seen for $T_7A_7N_7$. The adenines and thymines further away from the TA step have reduced cleavage. In fact, the minimum in cutting occurs around the AT step, which is lacking in both

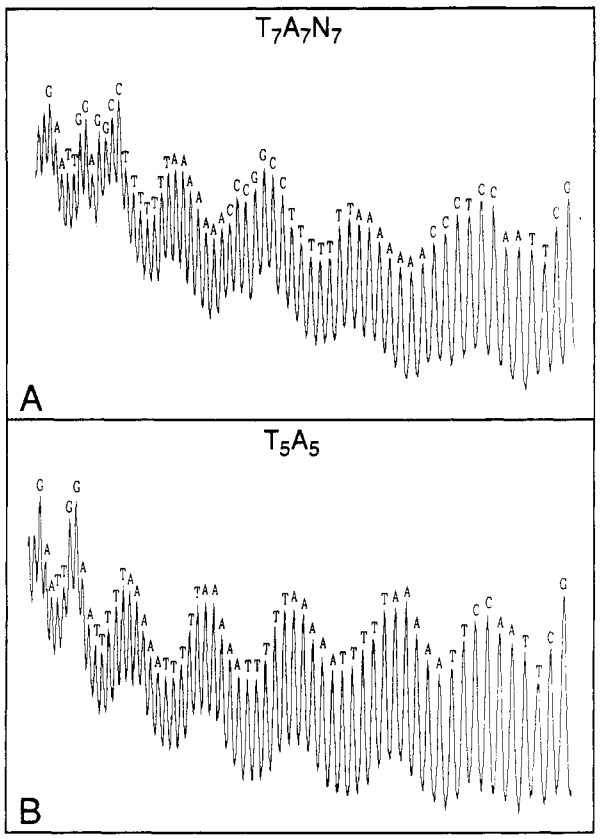

FIGURE 5: Densitometer scans of bent T_nA_n sequences. Panel A, the top strand of $T_7A_7N_7$; panel B, $(T_5A_5)_4$.

$T_7A_7N_7$ and $T_5A_5N_{11}$ because of the intervening N_7 and N_{11} tracts. Thus, regions of reduced susceptibility to cleavage by the hydroxyl radical around the AT step are interspersed with regions of normal susceptibility that surround the TA step, resulting in a sinusoidal pattern similar to that of A_5N_5.

Model for the Structures of T_nA_n Sequences. Previous models suggest that the structure of an adenine tract is the same whether it is in a bent or straight molecule. Our data show that the structure of an adenine tract depends on its sequence context. The bent T_nA_n sequences we have characterized with hydroxyl radical cleavage ($T_7A_7N_7$ and T_5A_5) have cutting patterns similar to that of the highly bent A_5N_5 sequence, in that there are periodic modulations in hydroxyl radical cleavage. The cutting patterns of all the bent sequences are modulated with a periodicity of approximately 10 nucleotides, as would be expected for a structural feature that affects DNA bending by occurring in phase with the DNA helix screw. In contrast, the T_5A_5 tract of $T_5A_5N_{11}$ (which runs with normal gel mobility) has a cutting pattern more similar to that of the straight T_nA_n sequence $T_4A_4N_2$, or to mixed-sequence DNA. The cutting patterns of T_nA_n tracts in *bent* sequences also show features found in the patterns of mixed-sequence DNA: that is, the central TA step and a few nucleotides to either side are cut to a similar extent as mixed-sequence DNA.

On the basis of the hydroxyl radical cleavage patterns of A-tract sequences, we have formulated a model for the structures of these sequences that also accounts for their bending properties. The model posits that in T_nA_n blocks the unusual adenine tract structure cannot form near the TA step, i.e., in the sequence TTAA or TTTAAA. However, outside the central core the normal adenine tract structure can form and, if phased properly, will cause a global bend in the DNA. In other words, we suggest that the T_3A_3 (or T_2A_2) core sequence behaves in its cleavage (and structural) properties as if it were mixed-sequence B-form DNA, which we denote as N_6 (or N_4).

For example, if we consider the T_3A_3 core sequence to be in the B-form structure, $T_4A_4N_2$ can be thought of as TN_6AN_2, and $T_5A_5N_{11}$ can be rewritten as $T_2N_6A_2N_{11}$. Since previous work has shown that at least four contiguous adenines are needed to induce bending, we propose that the reason these T_nA_n sequences are not bent is that they do not contain enough contiguous adenines outside the central core to form the unusual conformation seen in longer A-tracts (Koo et al., 1986; Diekmann, 1986).

How does our model explain bent T_nA_n sequences? We would rewrite the bent sequence $T_7A_7N_7$ as $T_4N_6A_4N_7$. We assert that this molecule is bent because even though the central T_3A_3 core cannot adopt the adenine tract conformation, the four contiguous adenines (and four contiguous thymines) flanking the core can. Thus, this sequence mimics one with alternating T_4 and A_4 tracts repeating every 10 or 11 bp. Previous work showed that a sequence with alternating T_5 and A_5 tracts phased at 10 bp intervals has the same mobility as a sequence with only A_5 tracts similarly disposed along the helix (Koo et al., 1986). Thus, we assume that $(T_4N_6A_4N_7)_n$ will be bent to a similar extent as repeating A_4 tracts phased with the helix screw. $(A_4N_6)_n$ was found to run on a gel with R_L^{150bp} (=mobility of a 150 bp fragment containing 15 repeats of the sequence/mobility of a "normal" DNA of 150 bp) $\approx$ 1.6 (Koo et al., 1986), while the R_L^{150bp} of $T_7A_7N_7$ is 1.67 (Haran & Crothers, 1989).

The bent sequence T_5A_5 (...$T_5A_5T_5A_5$...) (which has R_L^{150bp} = 1.55) would be considered by our model as ...$T_2N_6A_2T_2N_6A_2$.... The model explains the curvature of this sequence because A_2T_2, phased at 10 bp, is bent (R_L^{150bp} = 1.25) (Hagerman, 1988). We also note that the similarity of the cleavage patterns of $T_7A_7N_7$ and $(T_5A_5)_n$ (Figure 5) is consistent with the predictions of the model. The R_L^{150bp} values for $T_7A_7N_7$ and $(T_5A_5)_n$ are nearly the same, so these two sequences are presumably bent to a similar extent. Applying our model, we could write $(T_7A_7N_7)_n$ as ...$N_6A_4N_7T_4$...; similarly, $(T_5A_5)_n$ becomes ...$N_6(A_2T_2)N_6(A_2T_2)$.... This comparison shows that the A_4 (and T_4) tracts in $T_7A_7N_7$ adopt nearly the same phase and position in the sequence repeat as the A_2T_2 tracts in $(T_5A_5)_n$. Most models in the literature (including ours) posit that 5′-A–T-3′ steps act like A–A steps, so A_4 would be expected to be very similar to A_2T_2 in its structural properties.

Testing the Model. One requirement of the model is that the sequence $T_3A_3N_4$ have the structure of B-form DNA. While our cleavage results (Burkoff & Tullius, 1988; this work) with $T_4A_4N_2$ strongly suggest that this would be true, we have made a $T_3A_3N_4$ molecule (Figure 1A) and performed a hydroxyl radical cleavage experiment to test this presumption. The smooth cleavage pattern of $T_3A_3N_4$ (shown in Figures 2 and 4) is consistent with the model.

A stronger test of the model addresses the assertion that the T_3A_3 (or T_2A_2) core of *bent* T_nA_n sequences adopts the structure of mixed-sequence DNA. We decided to test this point directly by synthesizing two new A-tract sequences. We took the $T_7A_7N_7$ sequence and substituted 6 bp of mixed-sequence (N_6) for the T_3A_3 core. In another experiment, we substituted N_4 for the T_2A_2 core of $T_7A_7N_7$. These new sequences, $T_4N_6A_4N_7$ and $T_5N_4A_5N_7$, are shown in Figure 1A. We then used hydroxyl radical cleavage to compare the structures of the T_3A_3 and T_2A_2 cores of $T_7A_7N_7$ with the structures of mixed-sequence DNA in the same sequence

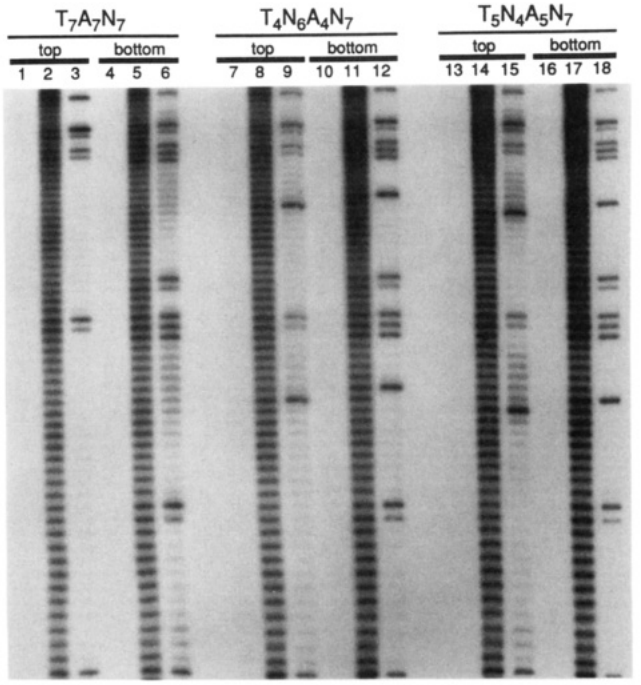

FIGURE 6: Autoradiograph of hydroxyl radical cleavage patterns of $T_7A_7N_7$ and substituted sequences. Lanes 1, 4, 7, 10, 13, and 16 contain untreated radiolabeled restriction fragments. Lanes 2, 5, 8, 11, 14, and 17 contain hydroxyl radical cleavage products. Lanes 3, 6, 9, 12, 15, and 18 contain the products of Maxam–Gilbert guanine-specific sequencing reactions run on the restriction fragments. Lanes 1–3, top strand of $T_7A_7N_7$; lanes 4–6, bottom strand of $T_7A_7N_7$; lanes 7–9, top strand of $T_4N_6A_4N_7$; lanes 10–12, bottom strand of $T_4N_6A_4N_7$; lanes 13–15, top strand of $T_5N_4A_5N_7$; lanes 16–18, bottom strand of $T_5N_4A_5N_7$.

context. To assess the degree of curvature of the new sequences, their electrophoretic mobilities were compared with the mobility of the parent $T_7A_7N_7$ sequence.

The sequences we chose for N_4, GTAC, and for N_6, GTATAC, are not as G/C-rich as N_7 in $T_7A_7N_7$ or N_{11} in $T_5A_5N_{11}$, both of which contain only guanine and cytosine. G/C-rich DNA may itself have an unusual structure (Drew & Travers, 1984), and certain G/C sequences can alter the bending properties of A-tracts (Milton et al., 1990a,b). We reasoned that including adenine and thymine in the N_4 and N_6 sequences would better approximate mixed-sequence B-form DNA.

Hydroxyl Radical Cleavage. The cleavage patterns of both strands of $T_4N_6A_4N_7$ are shown in the center of Figure 6, and the cutting patterns of both strands of $T_5N_4A_5N_7$ are shown at the right. For direct comparison, the corresponding cleavage patterns of both strands of $T_7A_7N_7$ are shown on the left in Figure 6. Densitometer scans of the cleavage patterns of the three sequences are presented in Figure 7. The cutting patterns of $T_4N_6A_4N_7$ and $T_5N_4A_5N_7$ closely resemble the cutting pattern of $T_7A_7N_7$ (compare panels B and C with panel A in Figure 7). That is, the sequences GTAC and GTATAC are cut to a similar extent as the T_2A_2 or T_3A_3 core of $T_7A_7N_7$. Furthermore, the A_4 and T_4 tracts in $T_4N_6A_4N_7$ and the A_5 and T_5 tracts in $T_5N_4A_5N_7$ have a decreased susceptibility to hydroxyl radical cleavage similar to the analogous adenines and thymines in the parent $T_7A_7N_7$ molecule. While it is difficult to determine from hydroxyl radical cleavage patterns exactly how many bp in the center of the T_nA_n tract are in the B-DNA conformation, the cleavage patterns in Figure 7 are consistent with the assertion that 4–6 bp around the TA step adopt a conformation similar to that of mixed-sequence DNA.

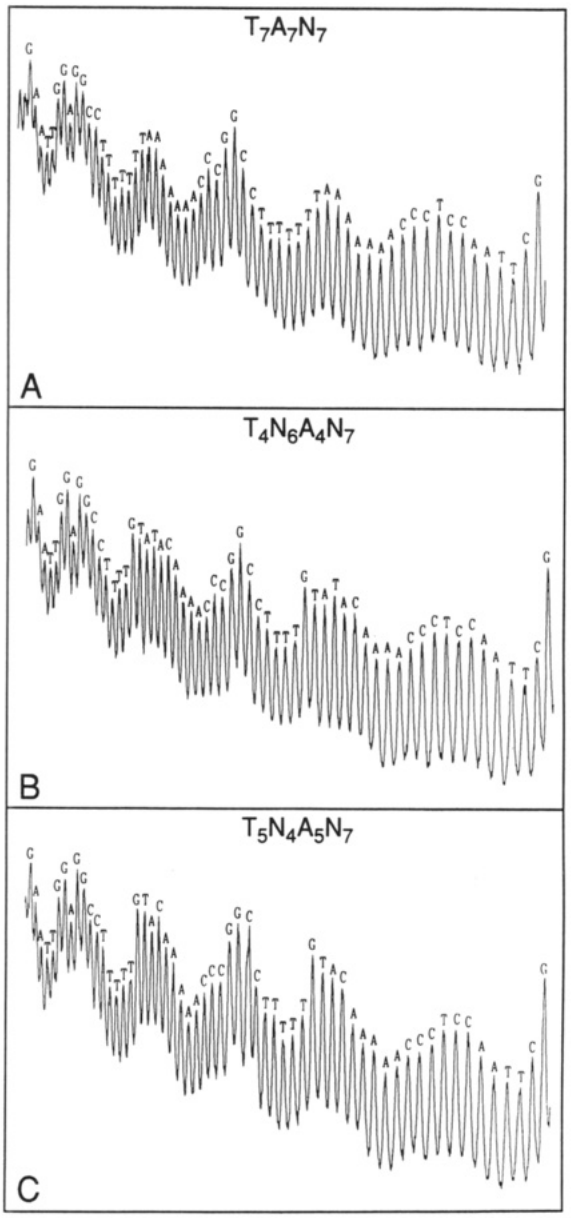

FIGURE 7: Densitometer scans of hydroxyl radical cleavage patterns of $T_7A_7N_7$ and substituted sequences. (A) Top strand of $T_7A_7N_7$; (B) top strand of $T_4N_6A_4N_7$; (C) top strand of $T_5N_4A_5N_7$.

Gel Mobility Determination. If the structure of the central core of a T_nA_n sequence is B-form, the mobility of $T_7A_7N_7$ should be similar to that of $T_4N_6A_4N_7$ and $T_5N_4A_5N_7$. The three 282 bp *Hin*dIII–*Pvu*II restriction fragments containing the inserted sequences (Figure 1) were electrophoresed on a native polyacrylamide gel to assay for bending (Figure 8). This assay is not strictly analogous to other mobility experiments in the literature, since our restriction fragments contain only two or four repeats of these sequences, and the inserted sequences are flanked by long arms (52 bp and 178 bp) contributed by the vector. Other experiments [for example, Haran and Crothers (1989), Koo et al. (1986), and Hagerman (1985)] tested the mobility of a ladder of fragments of various lengths containing only repeats of the sequence of interest. The results of such experiments are often succinctly summarized as R_L^{150bp} values. In Table I, we compare the apparent lengths we have determined for our 282 bp A-tract fragments (Figure 1) with the R_L^{150bp} values for these sequences collected from the literature. There is a good correlation between the values for each sequence derived from the two experiments.

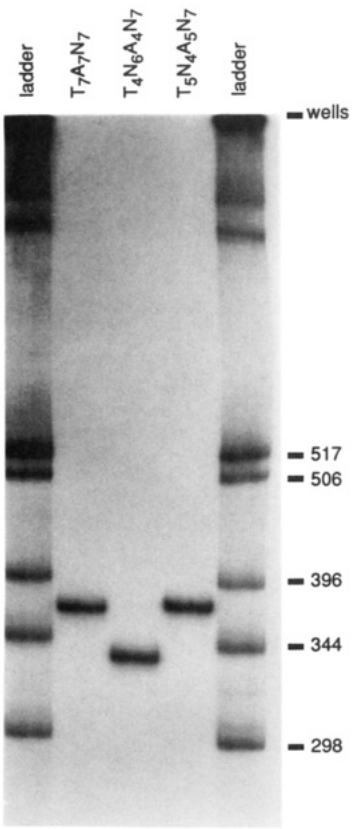

FIGURE 8: Electrophoretic gel mobility assay of $T_7A_7N_7$ and substituted sequences. Shown is an autoradiograph of an 8% nondenaturing gel (lanes 1 to 5 from left to right) on which was run 282 bp restriction fragments containing inserts of $T_7A_7N_7$ (lane 2), $T_4N_6A_4N_7$ (lane 3), and $T_5N_4A_5N_7$ (lane 4). All fragments are radiolabeled on the bottom strand. Lanes 1 and 5 contain radiolabeled size markers. The lengths of the size markers (in bp) are indicated to the right of the autoradiograph.

Table I: Anomalous Gel Mobility of T_nA_n Sequences

sequence	apparent length (bp)[a]	R_L [150bp b]
$T_3A_3N_4$	311	
$T_4A_4N_2$	323	1.05[c]
$T_5A_5N_{11}$	292	1.04[d]
$T_7A_7N_7$	380	1.67[d]
$T_4N_6A_4N_7$	343	
$T_5N_4A_5N_7$	384	
A_5N_5	408	2.07[e]
T_5A_5		1.55[f]

[a] The apparent length, as determined by electrophoretic mobility on an 8% polyacrylamide gel, of a 282 bp restriction fragment containing an insert of two or four repeats of the A-tract sequence near the center of the fragment. See Figure 1. [b] Ratio of the apparent length to the actual length of a 150 bp fragment consisting of repeats of the A-tract sequence. [c] Hagerman (1986). [d] Haran & Crothers (1989). [e] Koo et al. (1986). [f] Hagerman (1988).

This comparison demonstrates that the results of our gel mobility experiment provide similar information on bending as the ligation ladder experiment.

The mobility of $T_4N_6A_4N_7$ is slightly greater than $T_7A_7N_7$, but $T_5N_4A_5N_7$ runs nearly the same. All fragments are 282 bp; $T_4N_6A_4N_7$ migrates as if it were 343 bp; $T_7A_7N_7$, 380 bp; and $T_5N_4A_5N_7$, 384 bp (Table I). These data indicate that at the center of a T_nA_n sequence, a core sequence T_mA_m, with m between 2 and 3, adopts the B conformation. T_2A_2 seems to be the best approximation to the B-DNA region, since the gel mobility of $T_5N_4A_5N_7$ is closest to that of $T_7A_7N_7$.

Fourier Analysis of the Cleavage Patterns of $T_7A_7N_7$ and A_5N_5. The hydroxyl radical cleavage pattern of a set of phased adenine tracts interspersed with mixed-sequence DNA is sinusoidal (Burkhoff & Tullius, 1987). For $(A_5N_5)_n$, which has a sequence repeat of 10 bp, the period of this sinusoidal cleavage pattern is expected to be 10 nucleotides. Our model for the structure of T_nA_n sequences predicts for $T_7A_7N_7$ the formation of blocks of unusual conformation phased at ~10 bp, even though the repeat length of this sequence is 21 bp. This prediction is substantiated by the hydroxyl radical cutting pattern (Figure 5A), which shows decreased cutting at adenines and thymines away from the TA step.

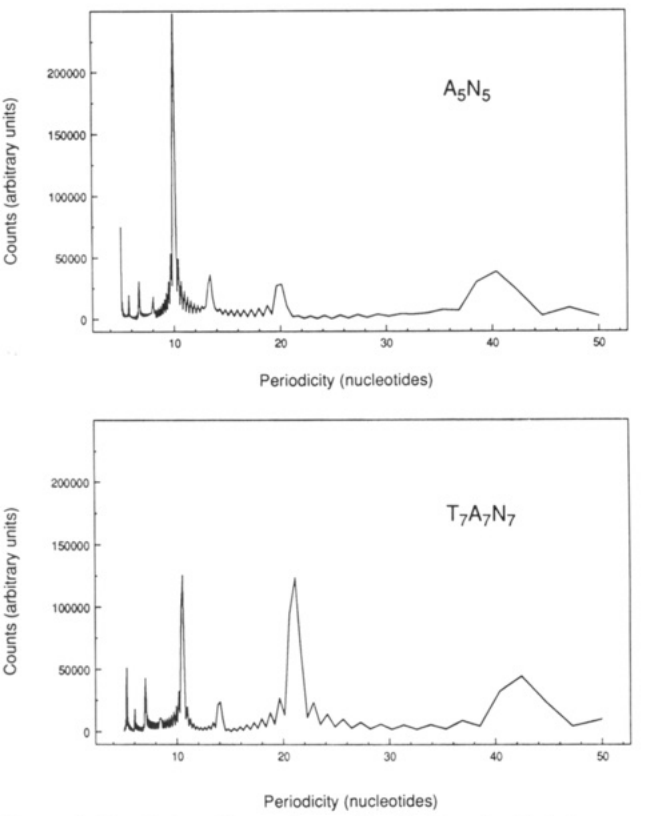

FIGURE 9: Fourier transforms of normalized hydroxyl radical cleavage data for A_5N_5 (top) and $T_7A_7N_7$ (bottom).

Because of recent success in the application of Fourier analysis for quantitative determination of periodicities in the hydroxyl radical cleavage patterns of DNA bound to calcium phosphate and to histones (Hayes et al., 1990, 1991), we used Fourier transformation as an objective means of quantifying the period and amplitude of the sine wave(s) in the hydroxyl radical cutting patterns of A-tract sequences. We performed Fourier transformations on the cleavage data for A_5N_5 and $T_7A_7N_7$. To lessen truncation artifacts in the Fourier transform, we constructed a larger data set by reiterating the cleavage data for a sequence. We justify this procedure by assuming that if we actually carried out the experiment on many repeats of the sequences, we would obtain the same peak integrals from repeat to repeat within experimental error.

Figure 9 shows the resulting Fourier transforms of the cleavage data for A_5N_5 and $T_7A_7N_7$. The transform of A_5N_5 has a large peak at a periodicity of 10 nucleotides, as expected. The transform of the $T_7A_7N_7$ pattern shows peaks at 10.5 (with height 0.6 times that of the peak of A_5N_5) and at 21 nucleotides. Thus, the Fourier transform reveals what is evident in the raw data for $T_7A_7N_7$, and confirms the prediction of our model: there is an unusual adenine tract structure which repeats with a periodicity (10.5 nucleotides) that is not evident in the sequence.

DISCUSSION

Hydroxyl Radical Cleavage Patterns of T_nA_n Sequences. Is our model for the structure of T_nA_n sequences consistent with the details of the hydroxyl radical cleavage patterns of these molecules? Cleavage data suggest that T_nA_n sequences have a different structure than A_n sequences that are surrounded by mixed-sequence DNA. Depending on the value of n, T_nA_n sequences can have features characteristic both of the unusual A-tract conformation and of B-form DNA. When $n = 3$ or 4, as in $T_3A_3N_4$ and $T_4A_4N_2$, as our model suggests, the structure is predominantly B-form: very little decrease in hydroxyl radical cleavage is seen in the adenine tract, and the A-tract appears to be cut at a level comparable to the surrounding DNA (Figure 4, panels A and B).

The sequence $T_5A_5N_{11}$ appears to be a borderline case. While the "$T_3A_3 = N_6$" version of our model would suggest that the T_5A_5 tract in $T_5A_5N_{11}$ will be predominantly B-form, like $T_3A_3N_4$ and $T_4A_4N_2$, the T_5A_5 tract *is* cut to a lesser extent compared to the N_{11} tract (Figure 4C). However, the data also show that the unusual structure of the A-tract in A_5N_5 is not adopted to the same extent in $T_5A_5N_{11}$ (compare the amplitudes of the cleavage patterns in Figure 3 and Figure 4C). Several phenomena likely contribute to this cutting pattern. The N_{11} sequence contains only G's and C's and therefore might itself have an unusual structure (Drew & Travers, 1984) that leads to increased hydroxyl radical cleavage, perhaps a wider than normal minor groove. The reduced hydroxyl radical cleavage we observe within the T_5A_5 tract indicates that this sequence adopts, to at least some extent, the unusual structure seen in other adenine tracts. However, within the T_5A_5 tract, a local maximum in cleavage does occur around the TA step (at the 3′-most T), similar to what is seen for the bent T_nA_n sequences $T_7A_7N_7$ and T_5A_5. Minima in cutting occur at the third T and at the 3′ end of the A-tract, similar to $T_7A_7N_7$.

If mixed-sequence DNA is substituted for TTAA instead of for TTTAAA (the "$T_2A_2 = N_4$" version of our model), $T_5A_5N_{11}$ can be thought of as $T_3N_4A_3N_{11}$. In this case, we would expect to see some decrease in cutting in the A_3 and T_3 tracts (Price and Tullius, unpublished observations), although A_3 tracts phased with the helix screw do not lead to appreciable electrophoretic anomaly (A_3N_7; Koo et al., 1986; Diekmann, 1986). Thus, the decreased cutting we see in $T_5A_5N_{11}$ is not inconsistent with our model. This explanation would fit with the suggestion that an unusual A-tract structure is formed in the $T_5A_5N_{11}$ sequence but the local bends that are produced are out-of-phase with the helix screw (Haran & Crothers, 1989).

Why is T_5A_5 bent? If we apply the model, $(T_5A_5)_n$ becomes $(T_2N_6A_2)_n$, which is the same as $(A_2T_2N_6)_n$. Hagerman (1988) has demonstrated by the gel mobility assay that this sequence is bent. Several methods (Coll et al., 1987; Burkhoff & Tullius, 1988; Leroy et al., 1988) have shown that 5′-AT-3′ steps do not interrupt the unusual conformation of an adenine tract. Detection of DNA bending by gel electrophoresis appears to require the presence of four contiguous A·T base pairs, possibly containing 5′-AT-3′ steps, but not 5′-TA-3′ steps (Crothers et al., 1990).

The local minimum in hydroxyl radical cleavage at the 5′ end of the T tract in T_5A_5 (Figure 5B) is consistent with the model. Cleavage of the 5′-most T in $T_5A_5N_{11}$, on the other hand, occurs to the same extent as cleavage of the 3′-T in this sequence, which reaches a local maximum in the pattern (Figure 4C). Molecular mechanics calculations suggest that the maximum in the minor groove width within the A-tract is shifted to the 3′ direction in T_5A_5 relative to A_5N_5 (Zhurkin et al., 1991), in agreement with hydroxyl radical cutting patterns and our model. That is, if the first two or three adenines at the 5′ end of the adenine tract of T_5A_5 are B-form, the location of unusual structure (and thus the decrease in hydroxyl radical cleavage) is shifted in the 3′ direction. We observe a maximum in hydroxyl radical cutting fairly consistently at the first two adenines, while the theoretical calculations show a maximum minor groove width at the second and third adenines (Zhurkin et al., 1991).

For $n = 7$, as in $T_7A_7N_7$, hydroxyl radical cleavage patterns (Figure 5A) again show decreases in cutting consistent with the model. As with T_5A_5, the unusual conformation begins further along the A-tract compared with A_5N_5. The first two adenines in $T_7A_7N_7$ are cleaved to a normal extent by hydroxyl radical; a significant decrease in cleavage does not occur until the third adenine. These data might suggest that the T_2A_2 rather than the T_3A_3 core sequence is B-form. The minimum in cleavage in the A-tract also is offset in the 3′ direction in $T_7A_7N_7$ relative to A_5N_5. The minimum in cutting in A_5N_5 is at the fourth adenine, while in $T_7A_7N_7$ it is at the sixth adenine. We feel that this is not simply because the A-tract is longer in $T_7A_7N_7$, because experiments on an A_{42} tract show that the minimum in hydroxyl radical cleavage is reached by the fourth adenine (Price and Tullius, unpublished observations).

Measurements of base pair lifetimes by NMR (Leroy et al., 1988) have provided additional structural information at the nucleotide level for T_nA_n sequences. A_n tracts with $n \geq 4$ and A_nT_n tracts with $n \geq 2$ were found to have anomalously low imino proton exchange rates compared with rates for A·T base pairs in mixed-sequence DNA. While the base pair lifetimes of T_4A_4 also were longer than normal, the lifetimes within the A_4 sequence of $N_2T_4A_4N_2$ were not as anomalous as those of the A_4 sequence in $N_3A_4N_3$. Similarly, the A_6 sequence in $N_2T_6A_6N_2$ had more normal lifetimes than the A_6 in $N_3A_6N_3$. These results suggest that A_n tracts in T_nA_n sequences are not equivalent in structure to A_n tracts surrounded by mixed-sequence DNA. In $N_3A_6N_3$, the longest base pair lifetime was found at the third A·T base pair (as it is in $N_3A_4N_3$ and $N_3A_5N_3$). In $N_2T_6A_6N_2$, however, the fourth and fifth A·T base pairs exhibited the longest lifetimes. These results mirror the hydroxyl radical cleavage pattern of $T_7A_7N_7$ and T_5A_5, which suggest that there is a shift to the 3′ direction of the start of the unusual structure in the A-tract of T_nA_n sequences compared to A_n tracts.

Fourier Analysis of the Cleavage Pattern of $T_7A_7N_7$. Fourier transformation of the cleavage data for $T_7A_7N_7$ offers further insight into the structure of this sequence. The regions of decreased cutting at the 5′ end of the T tracts and at the 3′ end of the A-tracts, separated by regions of normal cleavage frequency around the TA step and in the N_7 sequence, combine to give a cutting pattern for $T_7A_7N_7$ similar to that of A_5N_5. The appearance of a strong peak at ~10.5 nucleotides in the Fourier transform of the cleavage data of $T_7A_7N_7$ in addition to a peak at 21 nucleotides (the repeat length of the sequence) (Figure 9) confirms this idea quantitatively. This feature of the structure of $T_7A_7N_7$ also emerges from our model. We suggest that the phasing of the unusual structure at 10.5 bp adds to the bending of $(T_7A_7N_7)_n$. It is interesting to note that the peak at ~10.5 nucleotides in the Fourier transform of the $T_7A_7N_7$ pattern is less intense than the peak at 10 nucleotides in the A_5N_5 transform (Figure 9). Gel mobility experiments show that $T_7A_7N_7$ is not bent to the same extent as A_5N_5. We have found in a survey of many sequences that

there appears to be a correlation between the intensity of the Fourier peak at 10–10.5 nucleotides and the degree of anomalous gel mobility exhibited by the fragment (Price and Tullius, manuscript in preparation).

Comparison of $T_5N_4A_5N_7$ and $T_4N_6A_4N_7$ with $T_7A_7N_7$. The strongest evidence for our model comes from experiments on the molecules $T_5N_4A_5N_7$ and $T_4N_6A_4N_7$, in which the T_2A_2 or T_3A_3 core of $T_7A_7N_7$ has been substituted by mixed-sequence DNA (N_4 or N_6, respectively). The hydroxyl radical cutting patterns of the three sequences are quite similar (Figure 6), providing evidence that the model makes accurate local structural predictions. Equally striking is the gel mobility study. In an electrophoretic mobility experiment, $T_7A_7N_7$ behaves as if it were more bent than $T_4N_6A_4N_7$ but slightly less bent than $T_5N_4A_5N_7$ (Figure 7). Thus, the local structural descriptions we make in our model also accurately predict a global property of the molecule, macroscopic curvature.

Structural Basis of the Model. The cleavage pattern of A_5N_5 shows that adenine tracts surrounded by mixed-sequence DNA adopt an unusual conformation (Burkhoff & Tullius, 1987). The 3′ offset between the minima in hydroxyl radical cleavage in the adenine and thymine strands indicates that the experiment is sensitive to a feature of the minor groove. The reduction in cutting that is observed is likely due to reduced accessibility of the sugar residues upon narrowing of the minor groove (Burkhoff & Tullius, 1987).

Other methods have revealed that adenine tracts have unusual structural properties. The X-ray crystal structure of a dodecamer containing an A_6 tract at the center (Nelson et al., 1987) shows that the A·T base pairs are highly propeller-twisted, giving better purine stacking. This stacking interaction is expected to contribute considerably to the stability of the duplex (Levitt, 1978; Nelson et al., 1987). The extreme propeller twisting observed in the crystal structure is accompanied by formation of a series of bifurcated hydrogen bonds between O4 of thymine and N6 of adenine in the major groove, and narrowing of the minor groove (Nelson et al., 1987). NMR data also suggest that A-tracts have a narrow minor groove (Behling & Kearns, 1986; Kintenar et al., 1987; Katahira et al., 1988; Celda et al., 1989; Nadeau & Crothers, 1989). Recently, however, it has been shown that two structures are consistent with the NMR distance constraints (Chuprina et al., 1991). One is like the structure determined by crystallography, with highly propeller-twisted base pairs (~20°) and almost no tilt (Katahira et al., 1988), while the other exhibits smaller propeller twist (~10°) and negative tilt (~–7°) (Nadeau & Crothers, 1989).

When an A_4 tract follows a T_4 tract, as in $T_4A_4N_2$, the hydroxyl radical cutting pattern is fairly even, like mixed-sequence DNA, indicating that the unusual structure does not form. The model originally proposed by Burkhoff and Tullius (1988) suggested that steric clash in the minor groove at the TA step is relieved by damping the propeller twist, which in turn would widen the minor groove. Global structural properties (Hagerman, 1986) and the hydroxyl radical cutting pattern indicate that this effect propagates throughout the T_4A_4 sequence. The fact that $T_7A_7N_7$ is bent shows that the effect of the TA step does not extend for an unlimited distance. This is essentially what our model states: that the influence of the TA step is not infinite in extent [the domino effect referred to by Haran and Crothers (1989)], but dies off after 2–3 bp.

What might be the physical basis for our model? Consider an isolated T-tract and an isolated A-tract, each with highly propeller-twisted, well-stacked base pairs. If these two tracts are now juxtaposed to form a 5′-T_nA_n-3′ sequence, there will be a steric clash between the cross-strand adenines at the TA step (Calladine, 1982). This steric clash could be relieved by damping the propeller twist (Calladine, 1982; Chuprina, 1985, 1987; Burkhoff & Tullius, 1988). If the first (5′-most) adenine now has low propeller twist, it will no longer stack well with the second adenine if the second adenine is still highly propeller-twisted. The second adenine then also will dampen its propeller twist, but perhaps not quite as much as the first, and so on, until finally a base pair could have a high degree of propeller twist and can still be well stacked with the adjacent base pair.

We have suggested here that A·T base pairs in an A-tract are highly propeller-twisted, leading to a narrow minor groove. Some controversy remains as to whether this structure or the structure with negative tilt (Chuprina & Abagyan, 1988; Nadeau & Crothers, 1989; Crothers et al., 1989) is present in solution, since both structures are consistent with NMR distance constraints (Chuprina et al., 1991). If the highly tilted structure is correct, the arguments presented above would still apply. That is, the tilted structure also would result in a clash at the TA step, and one way to relieve this clash is for the DNA to adopt the B-form conformation around the TA step.

Implications of the Model. The difference between our model and the current junction model (Koo & Crothers, 1988; Haran & Crothers, 1989) lies in the prediction of when and where the unusual adenine tract conformation forms. For instance, for a sequence like $T_4A_4N_2$, using the junction model one would predict that both the thymine and adenine tracts are in an unusual conformation and that local bends occur at the T–A junction, the A–N junction, and the N–T junction. The junction model suggests that these bends cancel out, in agreement with the experimental observation that this sequence is not bent. Our model instead asserts that no unusual structure forms in this sequence, explaining the lack of global bending.

Assuming that bending occurs between tracts of unusual conformation and B-DNA, our model predicts that bends occur in different positions than does the current junction model. For $T_7A_7N_7$, the junction model suggests that local bends are at the same junctions as predicted for $T_4A_4N_2$ (i.e., at the hyphens in T_7-A_7-N_7-T_7), but in the case of $T_7A_7N_7$, these local bends add constructively rather than destructively and lead to global bending. Using the basic premise of the junction model and our predictions about where the unusual structure forms, on the other hand, we predict that local bends occur approximately where we have placed hyphens in the following sequence: N_7-T_5-T_2A_2-A_5-N_7. Since the presence and position of local bends are likely as important biologically as global bends, we feel that, although the revisions we make to the junction model are small changes, they are significant.

CONCLUSIONS

In this paper, we propose a model to describe the structures of T_nA_n sequences in DNA. We provide several pieces of evidence that support this model. Hydroxyl radical cleavage patterns show that the region around the TA step (T_3A_3 or T_2A_2) of such sequences is B-DNA-like but the unusual adenine tract structure does form outside of this core sequence. In the case of $T_7A_7N_7$, we showed that substitution of mixed-sequence DNA for the T_3A_3 or T_2A_2 core leads to a cutting pattern nearly identical to that of the original sequence. The new sequences also have nearly the same anomalous gel mobility as the original bent $T_7A_7N_7$ sequence. The details of the hydroxyl radical cutting patterns, and the electrophoretic mobility of $T_5N_4A_5N_7$ compared with $T_7A_7N_7$, lead to the

conclusion that the T_2A_2 core of a T_nA_n sequence most resembles B-form DNA. Finally, Fourier transformation of the hydroxyl radical cleavage pattern of $T_7A_7N_7$ confirms that an unusual structure occurs with a periodicity of 10.5 bp, as predicted by the model. The coincidence of the periodic repetition of this unusual structure with the helix screw of DNA helps explain why T_7A_7 is bent.

ACKNOWLEDGMENT

We thank Sarah Morse and Peter Kebbekus for synthesizing the oligonucleotides used in this work, Amy Kimball for many insightful comments on the manuscript, Judy Levin for suggesting the N_6 substitution experiment and for advice on cloning, and Jeff Hayes for assistance with the Fourier analysis.

REFERENCES

Alexeev, D., Lipanov, A., & Skuratovskii, I. (1987) *Nature 325*, 821–823.
Behling, R. W., & Kearns, D. R. (1986) *Biochemistry 25*, 3335–3346.
Burkhoff, A. M., & Tullius, T. D. (1987) *Cell 48*, 935–943.
Burkhoff, A. M., & Tullius, T. D. (1988) *Nature 331*, 455–457.
Calladine, C. R. (1982) *J. Mol. Biol. 161*, 343–352.
Celda, B., Widmer, H., Leupin, W., Chazin, W. J., Denny, W. A., & Wüthrich, K. (1989) *Biochemistry 28*, 1462–1471.
Chan, S. S., Breslauer, K. J., Hogan, M. E., & Kessler, D. J. (1990) *Biochemistry 29*, 6161–6171.
Chuprina, V. P. (1985) *FEBS Lett. 186*, 98–102.
Chuprina, V. P. (1987) *Nucleic Acids Res. 15*, 293–311.
Chuprina, V. P., & Abagyan, R. A. (1988) *J. Biomol. Struct. Dyn. 6*, 121–138.
Chuprina, V. P., Fedoroff, O. Y., & Reid, B. R. (1991) *Biochemistry 30*, 561–568.
Coll, M., Frederick, C. A., Wang, A.-H., & Rich, A. (1987) *Proc. Natl. Acad. Sci. U.S.A. 84*, 8385–8389.
Crothers, D. M., Haran, T. E., & Nadeau, J. G. (1990) *J. Biol. Chem. 265*, 7093–7096.
Dickerson, R. E. (1983) *J. Mol. Biol. 166*, 419–441.
Diekmann, S. (1986) *FEBS Lett. 195*, 53–56.
Diekmann, S. (1987) *Nucleic Acids Res. 15*, 247–265.
Diekmann, S., & Wang, J. C. (1985) *J. Mol. Biol. 186*, 1–11.
Drew, H. R., & Travers, A. A. (1984) *Cell 37*, 491–502.
Hagerman, P. J. (1985) *Biochemistry 24*, 7033–7037.
Hagerman, P. J. (1986) *Nature 321*, 449–450.
Hagerman, P. J. (1988) in *Unusual DNA Structures* (Wells, R. D., & Harvey, S. C., Eds.) pp 224–236, Springer-Verlag, New York.
Haran, T. E., & Crothers, D. M. (1989) *Biochemistry 28*, 2763–2767.
Hayes, J. J., Tullius, T. D., & Wolffe, A. (1990) *Proc. Natl. Acad. Sci. U.S.A. 87*, 7405–7409.
Hayes, J. J., Bashkin, J., Tullius, T. D., & Wolffe, A. P. (1991) *Biochemistry 30*, 8434–8440.
Herrera, J. E., & Chaires, J. B. (1989) *Biochemistry 28*, 1993–2000.
Katahira, M., Sugeta, H., Kyogoku, Y., Fuji, S., Fujisawa, T., & Tomita, K.-I. (1988) *Nucleic Acids Res. 16*, 8619–8632.
Kintanar, A., Klevit, R. E., & Reid, B. R. (1987) *Nucleic Acids Res. 15*, 5845–5863.
Koo, H.-S., & Crothers, D. M. (1988) *Proc. Natl. Acad. Sci. U.S.A. 85*, 1763–1767.
Koo, H.-S., Wu, H., & Crothers, D. M. (1986) *Nature 320*, 501–506.
Leroy, J.-L., Charretier, E., Kochoyan, M., & Gueron, M. (1988) *Biochemistry 27*, 8894–8898.
Levitt, M. (1978) *Proc. Natl. Acad. Sci. U.S.A. 75*, 640–644.
Lyamichev, V. (1991) *Nucleic Acids Res. 19*, 4491–4496.
Maniatis, T., Fritsch, E. F., & Sambrook, J. (1982) *Molecular Cloning: A Laboratory Manual*, Cold Spring Harbor Laboratory Press, Cold Spring Harbor, NY.
Marini, J. C., Levene, S. D., Crothers, D. M., & Englund, P. T. (1982) *Proc. Natl. Acad. Sci. U.S.A. 79*, 7664–7668.
Maxam, A. M., & Gilbert, W. (1980) *Methods Enzymol. 65*, 499–560.
Milton, D. L., Casper, M. L., & Gesteland, R. F. (1990a) *J. Mol. Biol. 213*, 135–140.
Milton, D. L., Casper, M. L., Wills, N. M., & Gesteland, R. F. (1990b) *Nucleic Acids Res. 18*, 817–820.
Nadeau, J. G., & Crothers, D. M. (1989) *Proc. Natl. Acad. Sci. U.S.A. 86*, 2622–2626.
Nelson, H. C. M., Finch, J. T., Luisi, B. F., & Klug, A. (1987) *Nature 330*, 221–226.
Park, Y. W., & Breslauer, K. J. (1991) *Proc. Natl. Acad. Sci. U.S.A. 88*, 1551–1555.
Sanger, F., Nicklen, S., & Coulson, A. R. (1977) *Proc. Natl. Acad. Sci. U.S.A. 74*, 5463.
Tullius, T. D., & Dombroski, B. A. (1985) *Science 230*, 679–681.
Ulanovsky, L. E., & Trifonov, E. N. (1987) *Nature 326*, 720–722.
Wing, R., Drew, H., Takano, T., Broka, C., Tanaka, K., Itakura, K., & Dickerson, R. E. (1980) *Nature 287*, 755–758.
Wu, H., & Crothers, D. M. (1984) *Nature 308*, 509–513.
Zhurkin, V. B., Ulyanov, N. B., Gorin, A. A., & Jernigan, R. L. (1991) *Proc. Natl. Acad. Sci. U.S.A. 88*, 7046–7050.